Articles

Contribution from the Department of Chemistry,
University of Durham, Durham DH1 3LE, England

An Extended Tensor Surface Harmonic Theory of Clusters

P. W. FOWLER* and W. W. PORTERFIELD†

Received November 12, 1984

The qualitative TSH theory, put forward by Stone, is used as a basis for an extended tensor surface harmonic (ETSH) calculation of the electronic structure and bonding in clusters. As in TSH, a cluster is treated as pseudospherical but in ETSH *individual* orbital energies are calculated, including σ–π interaction effects. We test the assumptions of TSH theory and find that whereas inclusion of σ–π interaction is *necessary* for correct electron counts, the tight-binding approximation does not lead to incorrect results. The results are compatible with Stone's qualitative TSH theory but are of extended Hückel accuracy. Energy levels of the correct number and (point group) degeneracy are obtained for boranes and polyhedranes, giving theoretical support for the empirical electron-counting rules and rationalizations of departures from them. TSH concepts thus expose the factors in the success of semiempirical EH and MNDO calculations on main-group clusters.

1. Introduction

Cluster compounds of main-group and transitional elements exercise a continuing fascination for experimental and theoretical chemists.[1,2] The most comprehensive qualitative description of bonding in clusters to date has been provided by Stone's tensor surface harmonic (TSH) theory.[3-6] This uses a free-electron molecular orbital approach to determine cluster wave functions and calculates *average* energies for groups of orbitals by using the simple Hückel approximations, assuming a spherical distribution of atoms in the cluster. TSH theory has several strong points. It yields analytical energy expressions from which it is possible to derive the empirical electron-counting rules[7-9] for boranes and transition-metal and other clusters. It rationalizes the prevalence of deltahedral structures. Most important of all, the pseudospherical symmetry labels give a language for the qualitative discussion of cluster bonding that may still be useful in interpreting more quantitative calculations.[10] The basic perception embodied in the TSH labeling of orbitals is that when counting nodes in the MOs we need to distinguish between nodes intrinsic to the component atomic orbitals and the nodes *between* atoms which determine the bonding characteristics of the orbital.

However, the simple form of TSH theory has some less desirable features. By grouping MOs of a given total angular momentum together in energy, it gives degeneracies higher than are actually present or possible in the orbital energies of real (nonspherical) clusters. An account of the splitting of these degeneracies would need to be added for a correct picture of most clusters. The TSH prediction of e.g. the Wade $n + 1$ rule for *closo*-boranes invokes σ–π interaction but without explicit calculation of its effects. In the absence of this interaction, too many bonding MOs would occur for the larger ($n > 10$) *closo*-boranes. Use of a tight-binding scheme for polyhedral clusters has also been criticized.[11]

Stone's TSH theory has found wide acceptance as a general, qualitative account of clusters. It is important, therefore, to investigate those features of the theory that produce the anomalies noted above and to correct them, where possible. That investigation is the main aim of the present paper.

Specifically, we construct a scheme based on the pseudospherical model of a cluster but avoid the further approximation of multiple degeneracies in the energy levels. This is done by calculating an energy for each individual orbital, rather than the weighted average energy used in ref 3–6. We take the MOs from the free-electron-on-a-sphere model problem but introduce σ–π interaction between them, as allowed even for a spherical cluster. Because we use the extended Hückel parameterization of the Hamiltonian,[11] the calculated energy levels show the correct degeneracies rather than the spuriously high degeneracies of the simple TSH expressions.[3] The end result is a demonstration that the basic assumptions of Stone's theory—that clusters are "spherical" and their MOs are harmonics—can be used to make *quantitative* predictions of electronic structure. Thus, numerical results at about the extended Hückel level of accuracy are obtained from a *guessed* wave function. The conceptual value of ETSH is that it exposes the reason for the success of EH,[12] MNDO,[10] and a variety of other methods in treating the systematics of main-group clusters.

In section 2 we give the mathematical structure of extended TSH theory and compare it to the original TSH theory of Stone.[3,4] Section 3 gives some practical details of calculations. Our results for the boranes are given in section 4 and for some polyhedral hydrocarbons are given in section 5. Extension to transition-metal clusters is discussed in section 6, and our conclusions are summarized in section 7.

2. Mathematical Aspects

In a conventional molecular orbital treatment of the bonding in clusters, wave functions are obtained as linear combinations of atomic orbitals, by finding the eigenvectors and eigenvalues of an electronic Hamiltonian. Free-electron molecular orbital (FEMO) models short-circuit this often lengthy computation by using the solutions of some particle-in-a-box problem to set the LCAO coefficients in advance. FEMOs from an appropriate model problem have the correct nodal structure and may be useful in qualitative discussions of bonding.

Stone uses the scalar, vector, and tensor surface harmonics, all of which may be derived from solutions for the free motion of an electron on a sphere,[3,13,14] to construct approximate cluster MOs.[3]

* Permanent address: Department of Chemistry, University of Exeter, Exeter EX4 4QD, England.
† Permanent address: Department of Chemistry, Hampden-Sydney College, Hampden-Sydney, VA 23943.

(1) Wilkinson, G., Stone, F. G. A., Abel, E. W., Eds. "Comprehensive Organometallic Chemistry"; Pergamon Press: Oxford, England, 1982.
(2) Johnson, B. F. G., Ed. "Transition Metal Clusters"; Wiley: New York, 1980.
(3) Stone, A. J. *Mol. Phys.* **1980**, *41*, 1339.
(4) Stone, A. J. *Inorg. Chem.* **1981**, *20*, 563.
(5) Stone, A. J.; Alderton, M. J. *Inorg. Chem.* **1982**, *21*, 2297.
(6) Stone, A. J. *Polyhedron* **1984**, *3*, 1299.
(7) Wade, K. *J. Chem. Soc. D* **1971**, 792.
(8) Wade, K. *Adv. Inorg. Chem. Radiochem.* **1976**, *18*, 1.
(9) Mingos, D. M. P. *Nature (London), Phys. Sci.* **1972**, *236*, 99.
(10) Brint, P.; Cronin, J. P.; Seward, E.; Whelan, T. *J. Chem. Soc., Dalton Trans.* **1983**, 975.
(11) Hoffmann, R.; Lipscomb, W. N. *J. Chem. Phys.* **1962**, *36*, 2179.
(12) Porterfield, W. W.; O'Neill, M. E.; Wade, K., in preparation.

0020-1669/85/1324-3511$01.50/0

This procedure generates an infinite, nonorthogonal, overcomplete set of functions from which a finite subset is to be selected. A summary of our version of the TSH calculation is presented in the current section.

In a main-group cluster, each (first-row) atom is assumed to contribute three basis functions to the skeletal bonding: one inward-pointing sp^x hybrid, σ_i, and two tangential p orbitals, π_i^θ and π_i^ϕ, directed along lines of longitude and latitude, respectively. Linear combinations of these functions give MOs of σ, π, and $\bar{\pi}$ type[3]

$$\chi_{lm}^{\sigma} = \sum_i C_{lm}(\theta_i,\phi_i)\sigma_i \tag{1}$$

$$\chi_{lm}^{\pi} = \sum_i V_{lm}^{\theta}(\theta_i,\phi_i)\pi_i^{\theta} + V_{lm}^{\phi}(\theta_i,\phi_i)\pi_i^{\phi} \tag{2}$$

$$\bar{\chi}_{lm}^{\pi} = \sum_i \bar{V}_{lm}^{\theta}(\theta_i,\phi_i)\pi_i^{\theta} + \bar{V}_{lm}^{\phi}(\theta_i,\phi_i)\pi_i^{\phi} \tag{3}$$

where the angular functions **C**, **V**, and $\bar{\mathbf{V}}$ are modified scalar, "even" and "odd" vector harmonics, respectively.[3] l and m are the usual angular momentum quantum numbers with $l = 0, 1, 2, \ldots$ for σ orbitals, but $l = 1, 2, \ldots$ for π and $\bar{\pi}$. Stone has tabulated the complex forms of **V** and $\bar{\mathbf{V}}$ for $l \leq 4$,[3] but we will use the real forms found by taking sin $m\phi$ and cos $m\phi$ combinations in place of $\exp(\pm in\phi)$.[15]

A finite cluster with a (σ,π) basis on each atom has $3n$ independent MOs. On physical grounds we retain the first n independent σ, π, and $\bar{\pi}$ orbitals, respectively (counted in order of increasing l), and discard the rest. The discarded functions are either null (i.e. vanish at all atomic sites) or linear combinations of the functions already counted. It is always necessary to discard some members of the highest allowed l shell for either σ or π. Problems can arise in Stone's original treatment if the discarded members are non-null as e.g. for the tetrahedral cluster.[4]

Individual orbital energies may be calculated for the approximate molecular orbitals. If the σ set is taken as an example, the energy of the (σlm) function is

$$W_{lm}^{\sigma} = \int \chi_{lm}^{\sigma *}\hat{F}\chi_{lm}^{\sigma}\, d\tau \Big/ \int \chi_{lm}^{\sigma *}\chi_{lm}^{\sigma}\, d\tau \tag{4}$$

where $\hat{F}$ is an effective one-electron Hamiltonian. If we substitute from (1) and abbreviate

$$F_{ij}^{\sigma} = \int \sigma_i^* \hat{F}\sigma_j\, d\tau \qquad F_{ii}^{\sigma} = \alpha^{\sigma}$$

$$S_{ij}^{\sigma} = \int \sigma_i^* \sigma_j d\tau \qquad S_{ii} = 1 \tag{5}$$

$$c_i = C_{lm}(\theta_i,\phi_i)$$

the energy becomes (for real wave functions)

$$W_{lm}^{\sigma} = (\alpha^{\sigma}\sum_i c_i^2 + 2\sum_{i<j} c_i c_j F_{ij}^{\sigma}) / (\sum_i c_i^2 + 2\sum_{i<j} c_i c_j S_{ij}) \tag{6}$$

Now if we introduce the extended Hückel parameterization of the Hamiltonian and set matrix elements of $\hat{F}$ from the corresponding overlaps[11]

$$F_{ij}^{\sigma} = \tfrac{1}{2}k(F_{ii}^{\sigma} + F_{jj}^{\sigma})S_{ij} = k\alpha^{\sigma}S_{ij} \tag{7}$$

where k is a constant parameter that is traditionally set to 1.75.[16] Thus

$$W_{lm}^{\sigma} = \alpha^{\sigma}(1 + kx_{lm}^{\sigma})/(1 + x_{lm}^{\sigma}) \tag{8}$$

where

$$x_{lm}^{\sigma} = 2\sum_{i<j} c_i c_j S_{ij} / \sum_i c_i^2 \tag{9}$$

In a similar way the π and $\bar{\pi}$ energies may be written in terms of dimensionless x parameters:

$$W_{lm}^{\pi} = \alpha^{\pi}(1 + kx_{lm}^{\pi})/(1 + x_{lm}^{\pi})$$
$$\bar{W}_{lm}^{\pi} = \alpha^{\pi}(1 + k\bar{x}_{lm}^{\pi})/(1 + \bar{x}_{lm}^{\pi}) \tag{10}$$

The x parameters have been introduced to give energy expressions formally similar to those in extended and simple Hückel theories.[11]

Even within the assumed spherical symmetry of the cluster, σ and π are not good quantum labels, because L^{σ} and L^{π} have the same symmetry and are mixed by the Hamiltonian. $\bar{L}^{\pi}$ sets are of opposite parity to L^{π} and therefore do not mix with σ or π functions in the spherical limit. As l and m (or l, $|m|$, and the sin/cos label for real functions) are conserved in spherical symmetry, the effect of σ–π interaction on the energies may be found by diagonalizing the 2×2 block of the Hamiltonian connecting χ_{lm}^{σ} and χ_{lm}^{π}

$$\begin{vmatrix} W_{lm}^{\sigma} - \epsilon & W^{\sigma\pi} - \epsilon S^{\sigma\pi} \\ W^{\sigma\pi} - \epsilon S^{\sigma\pi} & W_{lm}^{\pi} - \epsilon \end{vmatrix} = 0 \tag{11}$$

so that the final energies W_{lm}^{+} and W_{lm}^{-} are roots of a quadratic equation (+ denotes an energy lowered by the interaction and – an energy raised by the interaction). The energies W_{lm}^{+}, W_{lm}^{-}, and $\bar{W}_{lm}^{\pi}$ have taken into account *all* interactions allowed in the spherical symmetry group. For the real point group there may be further interactions as l and m are no longer good quantum numbers and as the π, $\bar{\pi}$ distinction becomes blurred, but these fall outside the scope of a TSH-type model.

The analysis developed so far differs in several important respects from Stone's original TSH theory.[3-6] The energies calculated from eq 1–11 relate to *individual* molecular orbitals where TSH would produce only *average* energies for each l shell. Although the coefficients of the wave function are chosen for a pseudospherical cluster, the actual (lower) molecular symmetry is reflected in the overlap matrix **S** and in the angles $\{\theta_i, \phi_i\}$. Therefore, the degeneracy pattern of the cluster MOs is the correct one for the molecular point group and is not the $2l + 1$ degeneracy of the spherical harmonics. Similarly, differences in radial distances are reflected in S so that the current treatment is expected to give results more or less compatible with extended Hückel calculations for a variety of polyhedra and to tolerate considerable departures from full spherical pseudosymmetry. Substitution of main-group heteroatoms into the cluster is another type of symmetry breaking that could be incorporated without difficulty.

Given a set of individual MO energies, it is possible to reconstruct the Stone average energies by taking the weighted sum[3]

$$W_l^{\lambda} = \sum_m W_{lm}^{\lambda} \int \chi_{lm}^{\lambda *}\chi_{lm}\, d\tau \Big/ \sum_m \int \chi_{lm}^{\lambda *}\chi_{lm}^{\lambda}\, d\tau \tag{12}$$

$$\lambda = \sigma, \pi, \bar{\pi}$$

In addition the average *after* σ–π interaction may be defined (λ = + and – in (12)), so that it is possible to take quantitative account of the interaction and check conclusions about the binding based on qualitative arguments.[3-6]

Stone's compact analytical expressions for the average energies without σ–π interaction[3] are made possible by two additional assumptions. The first is that of simple Hückel theory—counting only interactions between nearest neighbors. The second is to replace the angular separation ω_{ij} of any pair of neighbors by a single average angle. One of the major successes of TSH is the conclusion that "other things being equal" the most favorable structure for a cluster will be a deltahedron because this maximizes the number of nearest-neighbor interactions.[3,4] The qualification in the last sentence is an important one, since not all clusters adopt deltahedral structures. Furthermore, a naive application to *nido*-boranes would suggest that the "missing" vertex would be the one of lowest coordination number to maximize the number of remaining edges, and not the highest-coordinate vertex as observed and as predicted in TSH by more detailed but qualitative arguments.[5]

The prediction of *deltahedral* geometries rests on the simple Hückel or "tight-binding" approximation, which has been criticized by Hoffmann and Lipscomb.[11] The extended Hückel parameterization used in the present work includes both nearest-neighbor

(13) Redmond, D. B.; Quinn, C. M.; McKiernan, J. G. R. *J. Chem. Soc., Faraday Trans. 2* **1983**, *79*, 1791.
(14) Zhang, Q.-E. *THEOCHEM* **1984**, *109*, 215.
(15) Quinn, C. M.; McKiernan, J. G.; Redmond, D. B. *J. Chem. Educ.* **1984**, *61*, 572.
(16) Howell, J.; Rossi, A.; Wallace, D.; Haraki, K.; Hoffmann, R. *QCPE* **1977**, *11*, No. 344.

and cross-cage interactions and is not subject to the same criticism.[11]

In the present section we have shown how to modify the TSH calculation to give a new scheme (ETSH) for semiempirical calculation of molecular electronic structure. The results are expected to be of the extended Hückel type and to have the correct degeneracy but still remain within the conceptually useful TSH classification. Some applications to boranes and other clusters follow.

3. The Program

A computer program implementing the new ETSH treatment was written to interface with the standard FORTICON8[16] extended Hückel program. For any cluster two choices must be made: of coordinates and of σ, π basis. The origin of coordinates is fixed at the center of mass of the heavy atoms, and the z axis is the principal rotation axis of the molecular point group. Although exact MO results must be invariant under coordinate transformations, the TSH expressions contain an implicit dependence on the coordinate frame through the angles θ_i, ϕ_i.

Borane clusters $B_nH_n^{2-}$ contain strong two-electron B–H bonds which, to a first approximation, are not involved in skeletal bonding. Out of the 2s2p set on B, therefore, we project an exo sp hybrid to form the bond, leaving a σ endo sp hybrid and two π tangential p functions for skeletal bonding. This is similar to the in-surface-radial factorization of ref 11. Standard extended Hückel STO exponents and α parameters are used.

An overlap matrix is formed for the skeletal basis and the x^σ, x^π, and $\bar{x}^\pi$ parameters, and hence energies are calculated for all harmonics with $l \leq 3$. All 2×2 σ–π interaction matrices are diagonalized, yielding the final set of MO energies. Averages of the Stone type are also computed for each l shell before and after σ–π interaction.

A point that requires some discussion is the method of selecting just $3n$ MOs from the infinite TSH basis. Null functions are easily identified and cause no problem. For other cases, a criterion of linear independence is required. If each normalized candidate MO χ is written as a linear combination of the $3n$ basis functions $\{\Phi_i\}$

$$\chi_{lm}{}^{l} = \sum_{i=1}^{3n} a_i{}^{l}\Phi_i \qquad (13)$$

we can define a "scalar product" matrix

$$P_{IJ} = \sum_i a_i{}^{I} a_i{}^{J}$$

As one works up from low l, any function that is retained may be used to cast out higher l functions by reference to the **P** matrix. In general, functions with highest P_{IJ} are cast out until the appropriate number remain; this will sometimes entail retention of functions with P_{IJ} near 1 (though never ≥ 1), but the apparently low degree of independence does not seriously affect the resulting MO energies.

4. Boranes

We have carried out calculations of the skeletal MOs and orbital energies for the *closo*-boranes $B_nH_n^{2-}$ (n = 2, ..., 12) using the ETSH treatment. These molecules adopt deltahedral structures,[7] and for purposes of comparison we have idealized the geometries to *equilateral* polyhedra with R_{BB} = 170 pm and R_{BH} = 119 pm. Note that these are not particularly "spherical" clusters in some cases, e.g. for n = 11. Standard EH parameters and exponents were used. Our choice of σ sp hybrid leads to α^σ = −11.85 eV and α^π = −8.5 eV. Orbital energies from ETSH and EH calculations on these clusters are given in Table I. Before considering the results in detail, it is important to establish how far they are consistent with Stone's simple-Hückel, average-energy calculations. In Figures 1 and 2 the weighted average energies of each contributing l shell of MOs are plotted as a function of cluster size both before (Figure 1) and after (Figure 2) σ–π interaction. To facilitate comparison with Stone's graphs (Figures 1 and 2 in ref 3 or 2 and 6 in ref 4), the horizontal scale is $(\pi/\omega) - 1$, where ω is the average angular separation of nearest neighbors. The

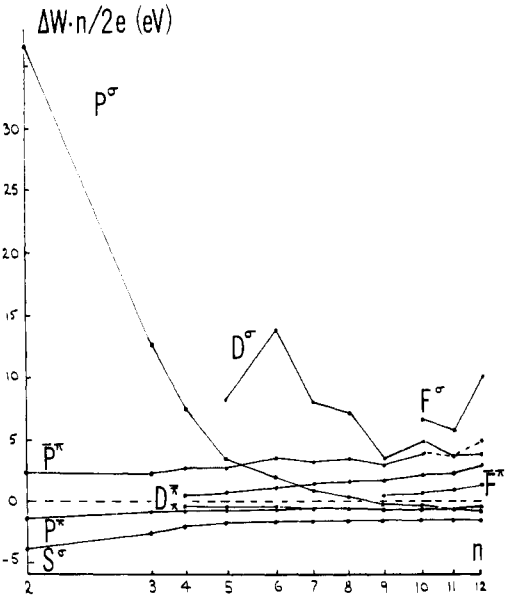

Figure 1. Energies of ETSH cluster MOs for *closo*-boranes in the average energy approximation without σ–π interaction. The F^π curve is hidden under P^σ and P^π but is an approximate reflection of $\bar{F}^\pi$ in the nonbonding line. See text for description of scales.

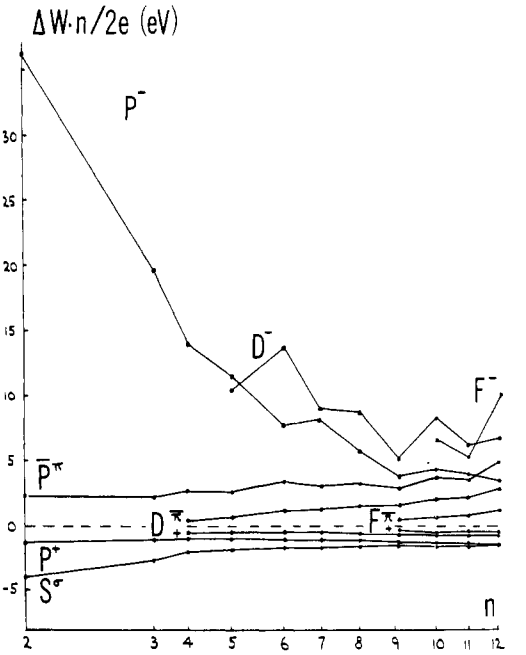

Figure 2. Energies of ETSH cluster MOs for *closo*-boranes in the average energy approximation including σ–π interaction. See text for discussion of scales.

scale is actually marked in terms of n for the equilateral deltahedra. The vertical scale is in eV and represents the bonding energy divided by the average coordination number of a vertex

$$y = (W^\lambda - \alpha^\lambda)/(2e/n)$$

where e is the number of edges of the polyhedron.

Considering first Figure 1, we see that our plot is essentially a discretization of the continuous curves which in ref 3 were obtained from analytical expressions. The ETSH approach includes all cross-cage interactions whereas the simple Hückel approximation used in ref 3 neglects them. The similarity of our Figure 1 and Stone's graphs is evidence for the view[17] that such interactions are not as important as has been implied in some recent models.[18]

(17) Housecroft, C. E.; Wade, K. *Inorg. Chem.* **1983**, *22*, 1391.
(18) Fuller, D. J.; Kepert, D. L. *Inorg. Chem.* **1983**, *21*, 163.

Table I. Comparison of ETSH and EH Energies for *closo*-Boranes[a]

$B_2H_2^{2-}$ ($D_{\infty h}$)			$B_3H_3^{2-}$ (D_{3h})			$B_4H_4^{2-}$ (T_d)		
EH		ETSH	EH		ETSH	EH		ETSH
−6.246 (×2)	$P_{\pm1}^{\pi}$	−6.246	−6.246 (×2)	$\bar{P}_{\pm1}^{\pi}$	−6.246	−8.704 (×2)	D_0^{π}, $\bar{D}_0^{\pi}$	−8.704
...	...	...	...	...	...	...	...	...
−9.820 (×2)	$P_{\pm1}^{+}$	−9.820	−10.492 (×2)	$P_{\pm1}^{+}$	−10.480	−11.304 (×3)	P^{+}	−11.384
−19.658	S^{σ}	−15.809	−10.687	P_0^{+}	−10.687	−21.885	S^{σ}	−17.909
			−20.940	S^{σ}	−17.148			

$B_5H_5^{2-}$ (D_{3h})			$B_6H_6^{2-}$ (O_h)			$B_7H_7^{2-}$ (D_{5h})		
EH		ETSH	EH		ETSH	EH		ETSH
−5.623 (×2)	$\bar{D}_{\pm1}^{\pi}$	−5.780	−3.726 (×3)	$\bar{D}_{\pm1-2}^{\sigma}$	−3.726	−4.439 (×2)	$\bar{D}_{\pm2}^{\pi}$	−4.439
...	...	...	...	...	...	...	...	...
−10.101 (×2)	$D_{\pm1}^{+}$	−10.096	−10.609 (×3)	$D_{\pm1-2}^{+}$	−10.609	−10.598 (×2)	$D_{\pm2}^{+}$	−10.675
−11.313 (×2)	$P_{\pm1}^{+}$	−11.403	−12.007 (×3)	P	−12.597	−10.705 (×2)	$D_{\pm1}^{+}$	−10.688
−12.509	P_0^{+}	−13.240	−22.906	S^{σ}	−18.575	−10.503*	P_0^{+}	−11.275
−22.447	S^{σ}	−18.246				−12.838 (×2)	$P_{\pm1}^{+}$	−13.981
						−23.228	S^{σ}	−18.690

$B_8H_8^{2-}$ (D_{2d})			$B_9H_9^{2-}$ (D_{3h})			$B_{10}H_{10}^{2-}$ (D_{4d})		
EH		ETSH	EH		ETSH	EH		ETSH
−6.838	$\bar{D}_{2c}^{\pi}$	−6.744	−6.865	$\bar{F}_{3c}^{\pi}$	−7.257	−4.790 (×2)	$\bar{F}_{\pm1}^{\pi}$	−5.315
...	...	...	...	...	...	...	...	...
−9.470	D_{2c}^{+}	−9.713	−9.301	F_{+3c}^{+}	−9.268	−9.870 (×2)	$F_{\pm1}^{+}$	−9.993
−10.613 (×2)	$D_{\pm1}^{+}$	−10.935	−10.732 (×2)	$D_{\pm1}^{+}$	−10.921	−10.855 (×2)	$D_{\pm1}^{+}$	−11.234
−11.36*	D_0^{+}	−11.133	−11.013 (×2)	$D_{\pm2}^{+}$	−11.409	−11.177 (×2)	$D_{\pm2}^{+}$	−11.297
−11.036	D_{2s}^{+}	−11.231	−11.369	D_0^{+}	−11.485	−12.051	D_0^{+}	−12.659
−12.182 (×2)	$P_{\pm1}^{+}$	−12.910	−12.189	P_0^{+}	−13.317	−12.564 (×2)	$P_{\pm1}^{+}$	−14.030
−13.105	P_0^{+}	−14.750	−12.927 (×2)	$P_{\pm1}^{+}$	−14.489	−13.156	P_0^{+}	−15.432
−23.438	S^{σ}	−18.824	−23.615	S^{σ}	−18.928	−23.775	S^{σ}	−18.990

$B_{11}H_{11}^{2-}$ (C_{2v})			$B_{12}H_{12}^{2-}$ (I_h)		
EH		ETSH	EH		ETSH
−6.133	$\bar{F}_{2s}^{\pi}$	−5.576	−2.499 (×4)	$\bar{F}_{\pm1\pm2}^{\pi}$	−2.449
...	...	...	...	...	...
−9.716	F^{+}	−10.087	−10.654 (×4)	$F_{\pm1\pm2}^{+}$	−10.654
−10.151		−10.151	−11.436 (×5)	D^{+}	−11.931
−10.329		−10.659	−13.187 (×3)	P^{+}	−15.511
−10.628	D^{+}	−11.192	−23.906	S^{σ}	−19.101
−11.026		−11.475			
−11.355		−11.551			
−11.502		−12.037			
−11.514		−12.067			
−12.219	P^{+}	−13.695			
−13.071		−14.892			
−13.492		−15.793			
−23.891	S^{σ}	−19.037			

[a] All energies are in eV, and degeneracies are indicated in parentheses. HOMO and LUMO levels are separated by the dotted line. Asterisks denote an ETSH MO out of the EH sequence. The cosine and sine harmonics are denoted by subscripts c and s or, for a degenerate pair, ±.

S^{σ} is always bonding. P^{σ} orbitals are initially highly antibonding but are bonding from $n \gtrsim 9$, dropping below P^{π} for $n \simeq 12$. The π levels are always bonding and coalesce for large n so that P^{π}, D^{π}, and F^{π} become indistinguishable on the scale of Figure 1. The high-energy $\bar{\pi}$ orbitals become more antibonding as n increases and are more widely spaced than π. The most dramatic feature of Figure 1 is the switch from highly antibonding to strongly bonding of P^{σ}, leading to apparently $n + 4$ bonding MOs for large n. Stone has argued[4] that the $n + 1$ rule is restored by considering σ–π interaction, and in Figure 2 we see that this is indeed the case. The main effect of the interaction is to push a P level out of the bonding set at large n, and incidentally to spread the energies of the other bonding orbitals.

Other treatments[11] have had the same problem of "extra" bonding orbitals when σ–π interaction is neglected, but this is the first explicit calculation of the effect demonstrating that σ–π interaction does indeed restore the electron count to the Wade's rule total for borane deltahedra.

After σ–π interaction the orbitals lose the pictorial simplicity of the surface harmonics. The W^{+} bonding combination of P^{σ} and P^{π} is mainly π in character for small n but becomes more σ-like as n increases. This change in character is at the root of the confusion over the correct labeling of the bonding P set.[10]

Figures 3 and 4 show the fully symmetry-split energy level patterns for the deltahedral boranes calculated by the ETSH method. For a given l the broad trend follows the average-energy curves of Figure 2, with bonding levels becoming more stable, and antibonding levels less stable, for increasing n. As the envelopes show, component sublevel energies oscillate with increasing amplitude about an average curve, coming together at clusters of high point group symmetry. Overlapping of the different l envelopes takes place for the highly antibonding W^{-} orbitals. The approximate mirror relationship between the π and $\bar{\pi}$ levels found in TSH theory[6] persists even after σ–π interaction and splitting of the spherical degeneracies as a relationship between the L^{+} and $\bar{L}^{\pi}$ energies. Thus we have a description of the bonding that follows Stone's theory in broad outline but gives more details of the energy level pattern.

Inspection of Figure 3 shows at once the advantage of calculating individual energies instead of the weighted averages. Consider the tetrahedral cluster. The $n + 1$ rule does not apply for $n = 4$: a tetrahedral cluster may use four bonding pairs as in B_4Cl_4 or six as in P_4. Our calculation shows that the $D_0^{\pi}/\bar{D}_0^{\pi}$ degenerate pair (E in T_d) is bonding by less than ~0.5 eV for a B_4 cage, and it is therefore reasonable either to occupy these orbitals as in P_4 or to leave them empty as in B_4Cl_4. This conclusion cannot be reached in the original TSH theory without "special pleading"[4] because (as Figure 2 shows) it predicts that D^{π} and $\bar{D}^{\pi}$ are split, one bonding and one antibonding. As Stone has explained,[4] the *average* energies are contaminated by con-

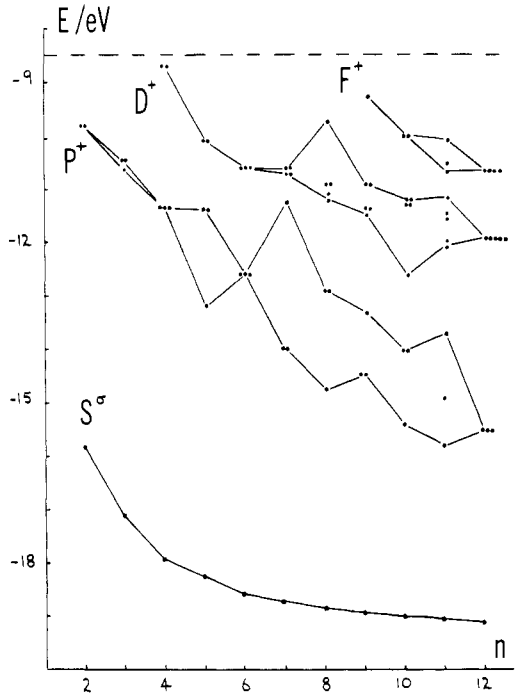

Figure 3. Energies of ETSH cluster MOs (bonding) for equilateral *n*-vertex *closo*-boranes. Degeneracies are represented by the appropriate number of dots.

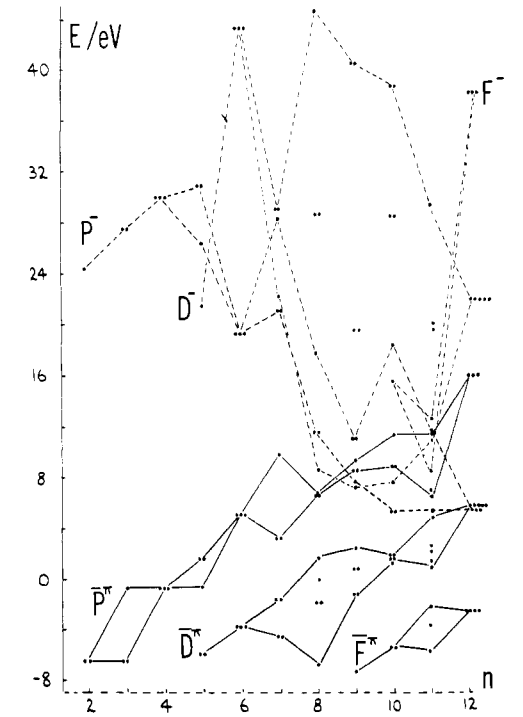

Figure 4. Energies of ETSH cluster MOs (antibonding) for equilateral *n*-vertex *closo*-boranes. Degeneracies are represented by the appropriate number of dots.

tributions from non-null but nonindependent P^{π} and $\bar{P}^{\pi}$ functions. In our approach these functions are discarded and the correct (degenerate) energies are found. Contamination of the same sort occurs for the highest, partly used *l* shell for $n = 5$, 9, 10, and 11 in the original TSH theory but does not change the electron count in these cases.

$n = 8$ and $n = 9$ clusters also have single, isolated energy levels near the nonbonding level. If these orbitals are filled, the cluster has $n + 1$ skeletal pairs as in $B_nH_n^{2-}$ but they can be left empty as in B_nCl_n or B_nBr_n. Our ETSH treatment is thus able to give a rationalization of the known stable polyhedral boron halides

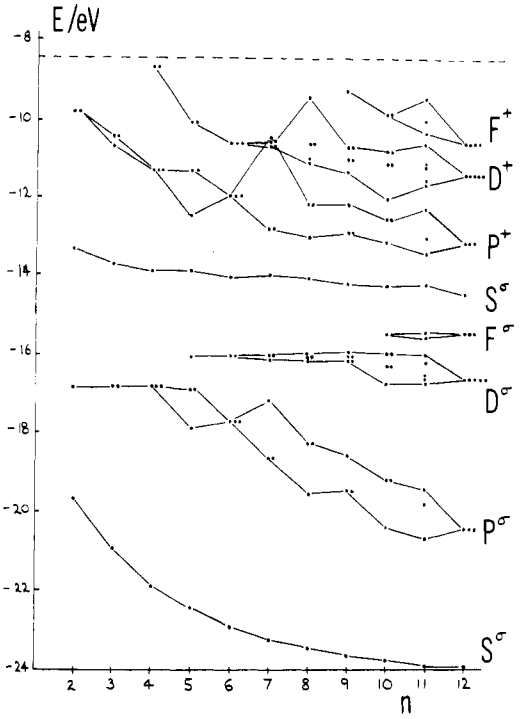

Figure 5. Energies of bonding MOs for the equilateral *n*-vertex *closo*-boranes in the extended Hückel approximation. TSH labels are used to classify the MOs. "Skeletal" and "BH" MOs are included. Compare Figure 3.

(B_4Cl_4, B_8Cl_8, B_9Cl_9, and B_9Br_9[19-22]) because it treats individual energy levels.

As we will see below, the one *closo*-borane where the ETSH and EH HOMOs differ is the $n = 7$ cluster. In EH a P_0 level lies ~0.2 eV *above* the $D_{\pm 2}^{+}$ doubly degenerate level so that the HOMO is nondegenerate. It is interesting to note, therefore, the existence of an unstable but *diamagnetic* species B_7Br_7.[23] On the other hand, our calculations predict that $B_{10}Br_{10}$[23] does not have a regular closo deltahedral structure.

The approximate mirror relationship between L^{+} and $\bar{L}^{\pi}$ energies suggests that the $n = 8$ and $n = 9$ clusters may also tolerate occupation of the low-lying nondegenerate antibonding orbital to give $n + 2$ skeletal pairs. Bi_9^{5+}[24] is an example of such a cluster. Wade and O'Neill have discussed the existence of closo clusters with *n*, $n + 1$, and $n + 2$ skeletal pairs in terms of the HOMO and LUMO degeneracies and commented on the unreliability of localized bond schemes in this connection.[25-27]

As the modified ETSH treatment uses the extended Hückel parameterization, it is desirable to compare the results with the exact eigenvalues of the same Hamiltonian by running an EH calculation. The EH procedure uses $5n$ atomic orbitals (B 2s, 2p, H 1s) and therefore generates $2n$ more MOs than the purely skeletal ETSH, σ, π, and $\bar{\pi}$ sets. The "extra" MOs are all of σ symmetry, resulting from addition of exo B hybrids and H 1s orbitals to the basis. We would expect to find *n* extra bonding and *n* antibonding MOs. Figure 5 shows the bonding MOs found by EH calculations on the *n*-vertex *closo*-boranes, grouped according to TSH labels. For purely formal electron-counting purposes the typical (i.e. $n \neq 4$) cluster has *n* BH bonding MOs

(19) Urry, G.; Wartik, T.; Schlesinger, H. I. *J. Am. Chem. Soc.* **1952**, *74*, 5809.
(20) Lanthier, G. F.; Massey, A. G. *J. Inorg. Nucl. Chem.* **1970**, *32*, 1807.
(21) Lanthier, G. F.; Kane, J.; Massey, A. G. *J. Inorg. Nucl. Chem.* **1971**, *33*, 1569.
(22) Reason, M. S.; Massey, A. G. *Inorg. Chem.* **1975**, *37*, 1593.
(23) Kutz, N. A. Morrison, J. A. *Inorg. Chem.* **1980**, *19*, 3295.
(24) Corbett, J. D. *Prog. Inorg. Chem.* **1976**, *21*, 140.
(25) O'Neill, M. E.; Wade, K. *Inorg. Chem.* **1982**, *21*, 461.
(26) O'Neill, M. E.; Wade, K. *THEOCHEM* **1983**, *103*, 259.
(27) O'Neill, M. E.; Wade, K. *Polyhedron* **1984**, *3*, 199.

and $n + 1$ skeletal bonding MOs. This turns out to be a fairly accurate description of the detailed composition of the MOs.

Inspection of the orbital composition indicates that the lower S^σ orbital is mainly a skeletal bonding combination of B 2s orbitals. It lies ~4 eV lower than the ETSH S because (i) it uses s rather than sp functions and (ii) it is pushed down by interaction with the S^σ combination of BH bonds. The lowest P set of MOs is dominated by terminal BH contributions for small n, but there is increased skeletal character mixed in for large n. Next come D and F sets, which are almost entirely BH bonding, followed by the BH bonding S. The next n MOs are almost pure skeletal bonding, except that the P set gains BH character for large n. Thus we have a general order of energies

$$\underset{1}{\text{S (skeletal)}} < \underset{n}{\text{P, D, F, S (BH)}} < \underset{n}{\text{P}^+, \text{D}^+, \text{F}^+ \text{ (skeletal)}}$$

with some ambiguity in the naming of the P sets. This description of the MO composition is consistent with Fenske–Hall approximate SCF,[28] MNDO,[10] and SCC[29] calculations on these clusters (the authors of ref 10 prefer to call the lowest P set skeletal). A similar order of skeletal and exo bonding MOs can be deduced from the EH calculations of Hoffmann and Lipscomb[11] on some of these clusters using $5n$, $4n$, and $3n$ basis functions. As we might expect for outward-pointing hybrids, the n dependence of the "BH" MO energies in Figure 5 is rather flat. Note that the natural S, P, D, F order of BH MOs is distorted by interaction with the skeletal sets but that the general shape of the curves for BH MOs is what would be expected from TSH theory.[3,10]

Table I gives skeletal MO eigenvalues in both EH and ETSH approaches. For each EH column the n orbitals above the lower S^σ are taken to be BH bonding and are omitted. In all cases the modified ETSH treatment gives the correct number and degeneracy pattern of MOs with only minor differences in order. The energies of the HOMO and LUMO levels usually match the exact calculation to within ~0.5 eV and, in high-symmetry cases, often give exact matches. Consequently the HOMO–LUMO energy separation is well modeled by ETSH. In high-symmetry cases, the composition of HOMO and LUMO is often determined by symmetry alone, e.g. for the D^π and $\bar{D}^\pi$ levels of $B_6H_6^{2-}$, and then EH and ETSH are in exact agreement. For any one cluster the match deteriorates as we move in either direction from the HOMO–LUMO gap. Three causes of numerical mismatch are (i) fixed sp hybridization, (ii) skeletal orbital mixings allowed within the point group but not in spherical symmetry, (iii) B–H terminal/skeletal orbital mixing. In the real cluster a different sp^x hybrid may be appropriate for each orbital and for each nonequivalent boron.[30] The HOMO/LUMO levels are often pure p in character (because the σ levels start at S^σ and "run out" first) and are therefore unaffected by this hybridization.

However, it is important to note that, for the practical purposes of understanding bonding, comparing stabilities, and counting electrons, the ETSH results are of about extended Hückel standard and that most of the numerical errors occur away from the critical HOMO/LUMO part of the MO diagram.

As discussed earlier, the quantitative inclusion of σ–π interaction is a crucial feature of our ETSH treatment. Two contrasting examples of the role of the interaction are given by $B_6H_6^{2-}$ and $B_{12}H_{12}^{2-}$. Figure 6 shows, for $B_6H_6^{2-}$, the MO diagram before and after interaction and illustrates the z components of P^σ and P^π sets. In octahedral $B_6H_6^{2-}$ the MO diagram is qualitatively the same before and after interaction. The only allowed interaction is between the bonding P^π set at −10.932 eV and the antibonding P^σ set at −4.200 eV, which are pushed apart to −12.597 and +19.252 eV, respectively. The HOMO and LUMO levels are unaffected, and the number of bonding MOs remains at 7.

For $B_{12}H_{12}^{2-}$, however, the picture is quite different. As Figure 7 shows, by the time the number of vertices has increased to 12,

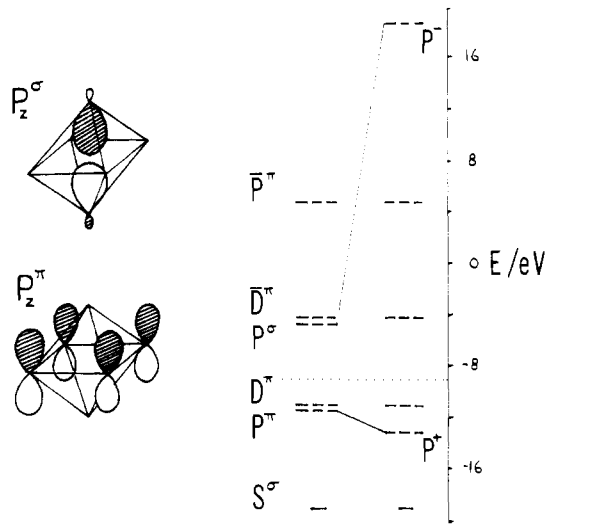

Figure 6. σ–π interaction for $B_6H_6^{2-}$. The MOs shown are z components of the P^σ and P^π sets before interaction. The MO energy diagram is shown before (left) and after (right) σ–π interaction.

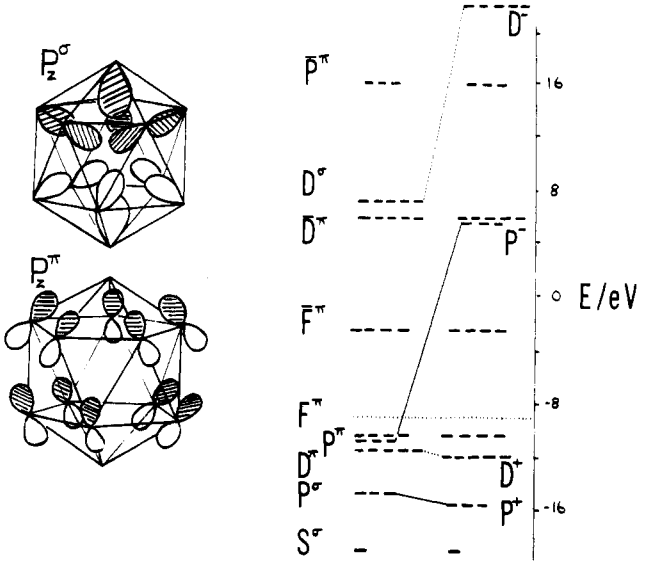

Figure 7. σ–π interaction for $B_{12}H_{12}^{2-}$. The MOs shown are z components of the P^σ and P^π sets before interaction. The MO energy diagram is shown before (left) and after (right) σ–π interaction.

both P^σ and P^π are bonding. Each P_z component has regions of bonding character (in the "tropics" of the pseudosphere) but is antibonding across the equator. Thus before interaction there are bonding P^σ (−14.826 eV) and P^π sets (−10.812 eV) leading to 16 bonding MOs. The allowed σ–π interactions are P^σ–P^π and D^σ–D^π, causing an unimportant stabilization of the D bonding set from −11.350 to −11.931 eV but ejecting a complete P set to 5.493 eV (where it is antibonding by 14 eV) and lowering P^+ to −15.511 eV. After interaction the bonding MO count is down to the correct 13.

Having shown that the modified TSH treatment gives very satisfactory results for the *closo*-boranes, we have applied the same method to some nido and arachno clusters. Stone[5] has given a qualitative discussion of the TSH model for these clusters by considering the changes in the spherical orbitals on abstraction of a vertex from a closo molecule. By comparing the open face to a conjugated system, he rationalizes the preference for nido clusters to be related to closo structures minus their highest coordinate vertex (HCV).[5] Similarly, the favored arachno structure has the largest open face, corresponding to removal of the HCV and a neighbor from a closo molecule. In both cases a larger open face is said to be preferred because it gives the most stable frontier orbitals.[5] It is worth pointing out that on this argument the arachno structure formed by removal of two *distant* HCVs may

(28) Stone, A. J., unpublished work.
(29) Pelin, W. K.; Spalding, T. R.; Brint, R. P. *J. Chem. Res., Synop.* **1982**, 120.
(30) Brint, R. P.; Pelin, K.; Spalding, T. *Inorg. Nucl. Chem. Lett.* **1980**, *16*, 391.

Table II. Comparison of ETSH and EH Energies for *nido*- and *arachno*-Boranes[a]

nido-Boranes

$B_6H_6^{4-}$ (C_{5v})			$B_6H_6^{4-}$ (C_{2v})			$B_5H_5^{4-}$ (C_{4v})		
EH		ETSH	EH		ETSH	EH		ETSH
−4.439 (×2)	$\bar{P}_{\pm1}{}^{\pi}$	−5.265	−4.439	$\bar{D}_0{}^{\pi}$	−4.045	−3.726	$\bar{D}_{-2s}{}^{\pi}$	−3.799
...	...	...	...	...	...	...	...	...
−9.604 (×2)	$D_{\pm1}{}^{+}$	−10.196	−8.544	$\bar{D}_{2c}{}^{\pi}$	−5.599	−9.200 (×2)	$D_{\pm1}{}^{+}$	−9.755
−10.598 (×2)	$D_{\pm2}{}^{+}$	−10.655	−9.147	$D_{1c}{}^{+}$	−8.136	−10.609	$\bar{D}_{+2c}{}^{\pi}$	−10.609
−10.711	$P_0{}^{+}$	−11.052	−10.467	$D_{1s}{}^{+}$	−9.947	−11.379	$P_0{}^{+}$	−11.408
−12.546 (×2)	$P_{\pm1}{}^{+}$	−13.595	−10.583	$D_{2s}{}^{+}$	−10.683	−11.749 (×2)	$P_{\pm1}{}^{+}$	−12.320
−22.547	S^{σ}	−18.256	−10.705	$P_{1s}{}^{+}$	−11.146	−22.336	S^{σ}	−18.209
			−12.312	$P_0{}^{+}$	−12.570			
			−12.767	$P_{1c}{}^{+}$	−13.825			
			−22.831	S^{σ}	−18.459			

arachno-$B_{10}H_{10}^{6-}$ (C_{2v})

EH		ETSH	EH		ETSH	EH		ETSH
−2.076	$\bar{F}_{-3s}{}^{\pi}$	−4.739	−11.014	$D_{+2}{}^{+}$	−11.230	−12.610	P^{+}	−14.951
...	...	...	−11.063		−11.565	−12.995		−15.310
−7.196	$D_0{}^{-}$	−5.233	−11.086		−11.727	−13.126		−16.853
−8.308	$P_0{}^{-}$	−6.920	−11.299		−11.910	−23.475	S^{σ}	−18.792
−9.858	$F_{2s}{}^{+}$	−10.310	−11.353		−12.987			
−10.525	$F_{3c}{}^{+}$	−10.611						

[a] See footnote *a* of Table I.

have a greater stabilization than when two neighbors are removed. For example, in $B_{10}H_{10}^{6-}$ the choice is between two five-membered rings and one six-membered ring. On simple Hückel grounds an isolated arachno structure would be preferred. Extended Hückel calculations have shown that for the bare $B_nH_n^{6-}$ arachno clusters the lowest energy isomers have isolated open faces.[12] It is only when the open faces are "stitched up" by bridging protons that the experimentally favored nearest-neighbor arachno isomer becomes the most stable in EH. Table II shows some results of an ETSH treatment of *nido* clusters. As before, the origin of coordinates is at the center of mass and the z axis along the principal axis of rotation.

Consider first the C_{4v} $B_5H_5^{4-}$ formed by removal of a vertex from octahedral $B_6H_6^{2-}$. The fit to EH results is as good as for a closo structure, reproducing the HOMO and LUMO, degeneracies, MO order, and, most important, the correct $n + 2$ orbital count in agreement with Wade's rules.[8] Also in Table II, we compare the $B_6H_6^{4-}$ clusters formed by abstraction of four- and five-coordinate vertices from the closo pentagonal bipyramid. In both extended Hückel and ETSH, the experimentally preferred C_{5v} structure has the lower total energy. The ETSH fit to the EH energy levels is still fairly good for the C_{5v} isomer but is very much worse for the C_{2v} unstable isomer. In particular the HOMO–LUMO gap is only half the EH value, making the electron count incorrect. On this limited evidence, it seems that a straightforward application of the modified TSH calculation can predict the correct nido structures, even though it gives a poorer quantitative fit to extended Hückel results. Selection of the orbitals to be discarded also becomes more difficult for nido structures where the $\pi/\bar{\pi}$ distinction is not so clear as for closo clusters.

When arachno isomers are considered, the results deteriorate further and, as the single example in Table II shows, are likely to be useless for predictions of structures.

That a TSH treatment based on the spherical group should fail for large arachno clusters is not surprising. As the nuclearity rises and symmetry elements disappear, the number of MOs belonging to the same symmetry species increases. Thus the number of interactions allowed by symmetry but ignored in TSH leads to a poorer fit for large, low-symmetry clusters. As we have seen, this is not a serious problem for *closo*-boranes but becomes acute for arachno clusters. For the same reason, it is possible that the TSH model will give a poor fit for larger "closo" clusters, although in the limit of *infinite* nuclearity spherical symmetry is regained.

In summary of this section, the extended TSH treatment gives a detailed picture of the bonding in *closo*-borane cages which is practically equivalent to an extended Hückel treatment but retains the conceptual simplicity of Stone's TSH theory. Useful results are also found for nido clusters, but the arachno clusters probably represent the limit of this treatment for boranes.

5. Applications: Electron-Precise Clusters

The electron-precise clusters C_nH_n form a class of compounds with an electron count different from that of boranes. They adopt structures based on three-connected polyhedra (tetrahedron, trigonal prism, cube, pentagonal prism, ..., pentagonal dodecahedron) held together by $3n/2$ skeletal electron pairs, one pair for each edge. Johnston and Mingos[31] have given a qualitative discussion of the original TSH theory for these compounds. In order to test whether our ETSH treatment is capable of reproducing the correct electron count and the detailed MO pattern of EH calculations for electron-precise as well as electron-deficient structures, we performed parallel ETSH and EH calculations (Table III). Since the known molecules of tetrahedrane, prismane, cubane, pentaprismane, and dodecahedrane have skeletons that are the duals of deltahedra, a plausible sequence of model geometries was found by taking duals of the borane deltahedra used in the borane calculations. All geometries were based on R_{CC} = 154 pm, R_{CH} = 114 pm (equilateral where possible). Standard EH parameters for carbon were used. As the pattern of energy levels rather than precise numerical detail is of interest here, sp hybrids were used as for boranes, leading to $\alpha^{\sigma} = -16.4$ eV, $\alpha^{\pi} = -11.4$ eV.

Table III shows that the ETSH theory predicts the correct electron count for structures through $C_{10}H_{10}$, and the numerical comparison with EH results is of the same quality as found for *closo*-boranes. Errors due to fixed hybridization are larger for carbon clusters but could be reduced by a more suitable choice of s, p mixture for the σ orbital. Again the errors are small at the HOMO/LUMO borderline. Note that the "extra" bonding orbitals come about by a lowering in energy of $(n - 2)/2$ of the n $\bar{\pi}$ MOs from antibonding (in deltahedra) to bonding (in three-connected polyhedra) to give a total count of $3n/2$ (see also ref 31). The versatile tetrahedron is both deltahedral and three-connected (also closo and nido). Its frontier orbitals show $\pi/\bar{\pi}$ mixing as discussed earlier.

It is gratifying, but perhaps not altogether surprising, that a theory based on the ideal spherical cluster should work well for the closed deltahedral and their duals, the three-connected polyhedra. *Planar* conjugated systems like benzene might be thought to be "insufficiently nearly spherical"[3] and to be beyond the scope of TSH theory. The results are of course well-known

(31) Johnston, R. L.; Mingos, D. M. P. *J. Organomet. Chem.* **1985**, *280*, 407.

Table III. Comparison of ETSH and EH Energies for Three-Connected Hydrocarbon Clusters[a]

C_4H_4 (T_d)			C_6H_6 (D_{3h})		
EH		ETSH	EH		ETSH
−4.335 (×3)	$\bar{P}^{\pi}$	−4.335	−6.155	P_0^{π}	−6.155
...	...	...	...	...	...
−11.948 (×2)	$D^{\pi}/\bar{D}^{\pi}$	−11.948	−11.688 (×2)	$D_{\pm 1}^{+}$	−11.929
−14.345 (×3)	P^{+}	−15.162	−12.882 (×2)	$\bar{D}_{\pm 1}^{\pi}$	−12.098
−29.532	S^{σ}	−24.354	−14.707*	D_0^{+}	−14.806
			−14.700 (×2)	$P_{\pm 1}^{+}$	−16.831
			−14.778	P_0^{+}	−18.204
			−30.469	S^{σ}	−24.874
C_8H_8 (O_h)			$C_{10}H_{10}$ (D_{5h})		
EH		ETSH	EH		ETSH
−1.686 (×3)	$\bar{P}^{\pi}$	−1.686	−2.091 (×2)	P	−3.742
...	...	...	...	...	...
−12.620 (×3)	D^{+}	−12.620	−11.827 (×2)	$\bar{F}_{\pm 2}^{\pi}$	−11.283
−12.118* (×3)	$\bar{D}^{\pi}$	−12.880	−12.515 (×2)	$\bar{D}_{\pm 1}^{\pi}$	−12.374
−15.098 (×2)	$D_{0,2c}^{+}$	−15.098	−12.941 (×2)	$F_{\pm 2}^{+}$	−12.757
−15.142 (×3)	P^{+}	−19.109	−13.125 (×2)	D^{+}	−14.506
−31.042	S^{σ}	−25.159	−15.135*		−15.174
			−14.811 (×2)		−15.808
			−15.239	P^{+}	−19.307
			−15.611 (×2)		−20.973
			−31.128	S^{σ}	−25.104

[a] See footnote *a* of Table I.

without TSH theory, but it is interesting to see how the Stone classification works for an example. For benzene our ETSH treatment leads to the correct configuration

$$(S^{\sigma})^2(P_{\pm 1}^{+})^4(D_{\pm 2}^{+})^4(F_{3c}^{\pi})^2(P_0^{\pi})^2(\bar{P}_{\pm 1}^{\pi})^4$$

with a degenerate LUMO $\bar{D}_{\pm 2}^{\pi}$ followed by $\bar{F}_{3c}^{\pi}$. Note that the presence of null and redundant functions in the D shell forces us to include F orbitals, which are necessary to provide an $|m| = 3$ function with the right number of nodes for fully antibonding orbitals. Thus ETSH theory can reproduce the Hückel-type orbitals of conjugated π systems that are far from spherical.

6. Transition-Metal Clusters

Stone has given a qualitative discussion of the application of his TSH ideas to transition-metal clusters[4,6] by considering all nine valence orbitals (s, p, d) on each metal atom. In principle, we could carry out an ETSH treatment along the same lines. A set of n atoms produces $3n$ σ, $2n$ π, and $2n$ $\bar{\pi}$, n δ, and n $\bar{\delta}$ orbitals. Interactions of two types, σ–π–δ and $\bar{\pi}$–$\bar{\delta}$, could be included by solving 6 × 6 and smaller matrices.

However, a smaller and simpler problem, more directly analogous to the treatment of boranes, can be envisaged if we use the isolobal analogy to guide the choice of basis functions. For example, a metal atom with three *exo*-CO ligands attached to it may be considered to use three orbitals in exo bonding and three for skeletal bonding, with three more occupied but effectively nonbonding.[8,9] Thus the effective basis for skeletal TSH calculations reduces to an sp^ad^b hybrid (σ) and two tangential pd^c (π) hybrids. This problem is no more difficult than the main-group calculation, differing only in using different hybrids. Other metal clusters with different ligand coordination require explicit consideration of δ orbitals.[32]

7. Conclusions

In this paper we have modified the original TSH theory to produce a practical scheme for calculations of the extended Hückel type. This allows us to test the various assumptions and approximations of the theory. The main points of the extended TSH treatment are (i) consideration of each orbital energy individually, (ii) use of an extended Hückel parameterization of the one-electron Hamiltonian, (iii) explicit calculation of σ–π interaction for each σlm, πlm pair, and (iv) a specific selection procedure for discarding redundant functions.

Results for boranes broadly confirm the qualitative conclusions of Stone, adding illuminating detail on deviations from Wade's rules, and are comparable in accuracy and utility to the full extended Hückel procedure. In particular our ETSH procedure gives energies of the correct point-group degeneracy and does not introduce spurious higher degeneracies. Furthermore, fairly drastic departures from pseudospherical symmetry are permitted. A brief discussion of benzene showed that the theory is not limited to deltahedra and their duals but can treat some planar systems.

Acknowledgment. W.W.P. thanks Hampden-Sydney College for a Faculty Fellowship enabling him to visit Durham University. We wish to thank Prof. K. Wade for his suggestions and interest in this work.

Registry No. $B_2H_2^{2-}$, 98105-14-7; $B_3H_3^{2-}$, 98105-15-8; $B_4H_4^{2-}$, 12429-81-1; $B_5H_5^{2-}$, 12429-90-2; $B_6H_6^{2-}$, 12429-97-9; $B_7H_7^{2-}$, 12430-07-8; $B_8H_8^{2-}$, 12430-13-6; $B_9H_9^{2-}$, 12430-24-9; $B_{10}H_{10}^{2-}$, 12356-12-6; $B_{11}H_{11}^{2-}$, 12430-44-3; $B_{12}H_{12}^{2-}$, 12356-13-7; tetrahedrane, 157-39-1; prismane, 650-42-0; cubane, 277-10-1; pentaprismane, 4572-17-2; dodecahedrane, 4493-23-6.

(32) Quinn, C. M.; McKiernan, J. G.; Redmond, D. B. *Inorg. Chem.* **1983**, *22*, 2310.